High-Redshift Quasars Found in Sloan Digital Sky Survey Commissioning Data II: The Spring Equatorial Stripe[1]

Xiaohui Fan[2], Michael A. Strauss[2], Donald P. Schneider[3], James E. Gunn[2], Robert H. Lupton[2], Scott F. Anderson[4], Wolfgang Voges[5], Bruce Margon[4], James Annis[6], Neta A. Bahcall[2], J. Brinkmann[7], Robert J. Brunner[8,9], Michael A. Carr[2], István Csabai[8,10], Mamoru Doi[11], Joshua A. Frieman[6,12], Masataka Fukugita[13,14], G. S. Hennessy[15], Robert B. Hindsley[15], Željko Ivezić[2], G. R. Knapp[2], D. Q. Lamb[12], Timothy A. McKay[16], Jeffrey A. Munn[17], Heidi Jo Newberg[6], A. George Pauls[2], Jeffrey R. Pier[17], Ron Rechenmacher[6], Gordon T. Richards[12], Constance M. Rockosi[12], Chris Stoughton[6], Alexander S. Szalay[8], Aniruddha R. Thakar[8], Douglas L. Tucker[6], Patrick Waddell[4], Donald G. York[12]

---

[1]Based on observations obtained with the Sloan Digital Sky Survey, and with the Apache Point Observatory 3.5-meter telescope, which is owned and operated by the Astrophysical Research Consortium.

[2]Princeton University Observatory, Princeton, NJ 08544

[3]Department of Astronomy and Astrophysics, The Pennsylvania State University, University Park, PA 16802

[4]University of Washington, Department of Astronomy, Box 351580, Seattle, WA 98195

[5]Max-Planck-Institut für extraterrestrische Physik, Postfach 1603, 85750 Garching, Germany

[6]Fermi National Accelerator Laboratory, P.O. Box 500, Batavia, IL 60510

[7]Apache Point Observatory, P.O. Box 59, Sunspot, NM 88349-0059

[8] Department of Physics and Astronomy, The Johns Hopkins University, 3701 San Martin Drive, Baltimore, MD 21218, USA

[9] Department of Astronomy, California Institute of Technology, Pasadena, CA 91125

[10]Department of Physics of Complex Systems, Eötvös University, Pázmány Péter sétány 1/A, Budapest, H-1117, Hungary

[11]Department of Astronomy and Research Center for the Early Universe, School of Science, University of Tokyo, Hongo, Bunkyo, Tokyo, 113-0033 Japan

[12]University of Chicago, Astronomy & Astrophysics Center, 5640 S. Ellis Ave., Chicago, IL 60637

[13]Institute for Cosmic Ray Research, University of Tokyo, Midori, Tanashi, Tokyo 188-8502, Japan

[14]Institute for Advanced Study, Olden Lane, Princeton, NJ 08540

[15]U.S. Naval Observatory, 3450 Massachusetts Ave., NW, Washington, DC 20392-5420

[16]University of Michigan, Department of Physics, 500 East University, Ann Arbor, MI 48109

[17]U.S. Naval Observatory, Flagstaff Station, P.O. Box 1149, Flagstaff, AZ 86002-1149

ABSTRACT

This is the second paper in a series aimed at finding high-redshift quasars from five-color ($u'g'r'i'z'$) imaging data taken along the Celestial Equator by the Sloan Digital Sky Survey (SDSS) during its commissioning phase. In this paper, we present 22 high-redshift quasars ($z > 3.6$) discovered from ~ 250 deg^2 of data in the spring Equatorial Stripe, plus photometry for two previously known high-redshift quasars in the same region of sky. Our success rate of identifying high-redshift quasars is 68%. Five of the newly discovered quasars have redshifts higher than 4.6 ($z = 4.62$, 4.69, 4.70, 4.92 and 5.03). All the quasars have $i^* < 20.2$ with absolute magnitude $-28.8 < \mathrm{M_B} < -26.1$ ($h = 0.5$, $q_0 = 0.5$). Several of the quasars show unusual emission and absorption features in their spectra, including an object at $z = 4.62$ without detectable emission lines, and a Broad Absorption Line (BAL) quasar at $z = 4.92$.

Subject headings: quasars: general; surveys

1. Introduction

This paper is the second in a series presenting high-redshift quasars selected from the commissioning data of the Sloan Digital Sky Survey (SDSS[18], York *et al.* 1999). In Paper I (Fan *et al.* 1999a), we presented the discovery of 15 quasars at $z > 3.6$ selected from two SDSS photometric runs covering ≈ 140 deg^2 in the Southern Galactic cap along the Celestial Equator observed in Fall 1998. In this paper, we describe observations of quasar candidates selected in a similar manner from 250 deg^2 of SDSS imaging data in the Northern Galactic cap, again along the Celestial Equator, observed in Spring 1999. The scientific objectives, photometric data reduction, selection criteria and spectroscopic observation procedures are described in Paper I, and will be outlined only briefly here.

We have not yet observed all the quasar candidates spectroscopically, so the objects described in these two papers do not form a complete sample. We will present the complete sample of high-redshift quasars found in the Equatorial stripe, and derive the quasar luminosity function at high redshift, in subsequent papers.

We describe the photometric observations and selection of quasar candidates briefly in §2. The spectra of 22 new high-redshift quasars are presented in §3.

[18] `http://www.astro.princeton.edu/PBOOK/welcome.htm`

2. Photometric Observations and Quasar Selection

The SDSS telescope (Siegmund *et al.* 1999[19]), imaging camera (Gunn *et al.* 1998), and photometric data reduction (Lupton *et al.* 1999b[20]) are described in Paper I. Briefly, the telescope, located at Apache Point Observatory in southeastern New Mexico, has a 2.5m primary mirror and a wide, essentially distortion-free field. The imaging camera contains thirty 2048×2048 photometric CCDs, which simultaneously observe 6 parallel $13'$ wide swaths, or *scanlines* of the sky, in 5 broad filters (u', g', r', i', and z') covering the entire optical band from the atmospheric cutoff in the blue to the silicon sensitivity cutoff in the red (Fukugita *et al.* 1996). The photometric data are taken in time-delay and integrate (TDI, or "drift-scan") mode at sidereal rate; a given point on the sky passes through each of the five filters in succession. The total integration time per filter is 54.1 seconds. The data were calibrated photometrically by observing secondary standards in the survey area using a (now decommissioned) 60cm telescope at Apache Point Observatory and the US Naval Observatory's 1m telescope. The photometric calibration used in this paper is only accurate to 5–10%, due to systematics in the shape of the point spread function across individual CCDs, and the fact that the primary standard star network had not yet been finalized at the time of these observations. This situation will be improved to the survey requirement of 2% in future papers in this series. Thus as in Paper I, we will denote the preliminary SDSS magnitudes presented here as u^*, g^*, r^*, i^* and z^*, rather than the notation u', g', r', i' and z' that will be used for the final SDSS photometry.

In this paper, we select quasar candidates from four SDSS imaging runs in the Northern Galactic Cap. The data were acquired with the telescope parked at the Celestial Equator. Details of the photometric runs are summarized in Table 1. Two interleaved SDSS scans, or the Northern and Southern *strips*, form a filled *stripe* 2.5 degrees wide in declination, centered on the Celestial Equator. Run 77 and 745 cover the Northern strip of the Equatorial Stripe, while Runs 85 and 752 cover the Southern strip. Runs 77 and 745, and runs 85 and 752 have considerable overlap, but candidates were selected only on the catalogs based on individual runs. The total stripe is roughly 7 hours long and covers a total area of about 250 deg^2 at Galactic latitude in the range $25° < b < 63°$. All four nights were photometric, with seeing conditions varying from $1.3''$ to worse than $2''$.

The data are processed by a series of automated pipelines to carry out astrometric and photometric measurements (c.f. Paper I, and references therein). The final object catalog

[19]see also `http://www.astro.princeton.edu/PBOOK/telescop/telescop.htm`

[20]see also `http://www.astro.princeton.edu/PBOOK/datasys/datasys.htm`

includes roughly 5 million objects in total. The limiting magnitudes are similar to those of Paper I, roughly 22.3, 22.6, 22.7, 22.4 and 20.5 in u^*, g^*, r^*, i^* and z^*, respectively. Figure 1 presents the color-color diagrams from Run 752 for all stellar sources at $i^* < 20.2$. The inner parts of the diagrams are shown as contours, linearly spaced in density of stars per unit area in color-color space. As in Paper I, a source is plotted only if it is detected in all three of the relevant bands at more than 5σ. In addition, objects that are flagged as saturated, lying on the bleed trail of a saturated star, overlapping the edge of the image boundary, or showing other indications of possible problems in the photometric measurement, are rejected. The median tracks of quasar colors as a function of redshift, as well as the locations of low-redshift ($z < 2.5$) quasars, hot white dwarfs and A stars, all from the simulation of Fan (1999), are also plotted in Figure 1.

High-redshift quasar candidates were selected using color cuts similar to those presented in Paper I. Because of the uncertainties in the photometric zeropoints, we found that the stellar locus shifted by of order 0.05 mag in the color-color diagrams between the Fall (Paper I) and Spring observations. We adjust the color cuts presented in Paper I according to these shifts. Final color cuts of the complete sample will be presented in a later paper with the final photometric calibrations. The color selection criteria used in this paper are as follows:

1. gri candidates, selected principally from the $g^* - r^*, r^* - i^*$ diagram:

$$\begin{aligned} &(a)\ i^* < 20 \\ &(b)\ u^* - g^* > 2.0 \text{ or } u^* > 22.3 \\ &(c)\ g^* - r^* > 1.0 \\ &(d)\ r^* - i^* < 0.08 + 0.42(g^* - r^* - 0.96) \text{ or } g^* - r^* > 2.26 \\ &(e)\ i^* - z^* < 0.25 \end{aligned} \tag{1}$$

2. riz candidates, selected principally from the $r^* - i^*, i^* - z^*$ diagram:

$$\begin{aligned} &(a)\ i^* < 20.2 \\ &(b)\ u^* > 22.3 \\ &(c)\ g^* > 22.6 \\ &(d)\ r^* - i^* > 0.8 \\ &(e)\ i^* - z^* < 0.47(r^* - i^* - 0.68) \end{aligned} \tag{2}$$

The intersections of those color cuts with the $g^* - r^*, r^* - i^*$ and $r^* - i^*, i^* - z^*$ diagrams are illustrated in Figure 1. A total of 80 gri and riz candidates that have colors consistent with quasars at $z > 3.6$ and $i^* < 20.0$ were selected from the catalog.

Several other *riz* candidates ($z > 4.6$) at $i^* < 20.2$ were also selected and observed. Two of the candidates, SDSSp J105320.43–001649.3 and SDSSp J111246.30+004957.5 (see Table 2; for naming convention, see §3), are the previously known quasars BRI1050–0000 ($z = 4.29$, Storrie-Lombardi *et al.* 1996) and BRI1110+0106 ($z = 3.92$, Smith, Thompson & Djorgovski 1994). Those two objects are the only quasars with $z > 3.6$ in the area covered in the NED database[21].

3. Spectroscopic Observations

Spectra of 32 high-redshift quasar candidates from the Equatorial Stripe were obtained with the ARC 3.5m telescope of the Apache Point Observatory, using the Double Imaging Spectrograph (DIS), during a number of nights from March to May 1999. Exposure times of these candidates range from 600 seconds for the brightest ($i^* \sim 17$) candidate to 5400 seconds for the faintest candidates. The instrument and spectral data reduction procedures were described in Paper I. The final spectra extend from 4000 Å to 10000 Å, with a spectral resolution of 12 Å in the blue and 14 Å in the red. They have been flux calibrated and corrected for telluric absorption with observations of F subdwarfs (Oke & Gunn 1983, Oke 1990). Twenty-one of the candidates are identified to be high-redshift quasars at $z > 3.6$. In particular, five of the candidates are quasars at $z > 4.6$, with redshifts of 4.62, 4.69, 4.70, 4.92 and 5.03, respectively. Two of these objects have very unusual spectra. SDSSp J153259.96–003944.1 is identified as a quasar without detectable emission lines at $z = 4.62$. Its optical, radio, and polarization properties are reported in a separate paper (Fan *et al.* 1999b). SDSSp J160501.21–011220.0 is a Broad Absorption Line (BAL) quasar at a redshift of 4.92 with two BAL systems, and is described further below. One additional object, SDSSp J130348.94+002010.4, was also observed. It has redder $g^* - r^*$ and $r^* - i^*$ colors than required by our color selection criteria (eq. 1), but is identified as a BAL quasar at $z = 3.64$. We present its spectrum below but will not include it in the future statistical analyses.

Table 2 gives the position and SDSS photometry, the redshift of each confirmed SDSS quasar and the photometric run from which it was selected. For the objects in the overlap region between runs, only the results from the runs from which they are selected are listed. None of these quasars show magnitude differences of more than 0.2 mag in the high signal-to-noise passbands between runs. We also include the SDSS measurements of the

[21]The NASA/IPAC Extragalactic Database (NED) is operated by the Jet Propulsion Laboratory, California Institute of Technology, under contract with the National Aeronautics and Space Administration.

two previously known $z > 3.6$ quasars in Table 2. The naming convention for the SDSS sources is SDSSp J HHMMSS.SS±DDMMSS.S, where "p" stands for the preliminary SDSS astrometry, and the positions are expressed in J2000.0 coordinates. The preliminary SDSS astrometry is accurate to better than $0.2''$ in each axis. The photometry is expressed in asinh magnitudes (Lupton, Gunn & Szalay 1999, see also Paper I); this magnitude system approaches normal logarithmic magnitudes at high signal-to-noise ratio, but becomes a linear flux scale for low signal-to-noise ratio, even for slightly negative fluxes. The photometric errors given are statistical in nature and do not include the systematic errors due to PSF variation across the field and uncertainties in the photometric zeropoint. Positions of the 24 confirmed SDSS quasars on the color-color diagrams are plotted on Figure 1. Finding charts of all objects in Table 2 are given in Figure 2. They are $200'' \times 200''$ i' band SDSS images with an effective exposure time of 54.1 seconds.

We matched the positions of quasars in Table 2 against radio surveys. Twenty of them are in the region covered by the FIRST survey (Becker, White & Helfand 1995). Three of them have FIRST counterparts at 20 cm at the 1 mJy level (with positional matches better than $1''$). Two new SDSS quasars, SDSSp J123503.04–000331.8 ($z = 4.69$) and SDSSp J141205.78–010152.6 ($z = 3.73$), correspond to FIRST sources of 18.4 and 4.3 mJy at 20 cm, respectively. One of the previously known quasars, SDSSp J105320.43–001649.3 (BRI1050-0000, $z = 4.29$), is also a FIRST source of 13.8 mJy. The three quasars with RA $> 16^h$ are not covered by the FIRST survey. We matched them against the NVSS survey (Condon *et al.* 1998); none of them has an NVSS counterpart at 20cm at the 2.5 mJy level.

We have similarly cross-correlated the list against the ROSAT full-sky pixel images (Voges *et al.* 1999); none of these objects were detected, implying a typical 3-σ upper limit of 3×10^{-13}erg cm^{-2}s^{-1} in the 0.1 – 2.4 keV band. This result is not unexpected; only a few $z > 4$ quasars have an observed X-ray flux above this value (e.g. Fabian *et al.* 1997, Moran & Helfand 1997), and the typical X-ray flux from known optically selected $z > 4$ quasars is a factor of four or more lower than our limit (Brandt 1999). We expect positive ROSAT X-ray detections of a substantial fraction of the somewhat brighter, lower-redshift quasars in the SDSS.

Among the 34 observed candidates which satisfy Equations 1 and 2 (including the two previously known quasars), 23 are confirmed as quasars at $z > 3.6$, a success rate of 68%, similar to the success rate we reported in Paper I. Ten of the eleven non-quasars are faint late type stars, which are typical contaminants of high-redshift quasar searches. One of the candidates, however, has spectral features that we have not yet been able to identify; we will present its spectrum and discuss possible explanations in a separate paper.

Figure 3 presents our spectra of the 22 new SDSS quasars. In Figure 3, we place

the spectra on an absolute flux scale (to compensate for the uncertainties due to non-photometric conditions and variable seeing during the night) by forcing the synthetic i^* magnitudes from the spectra to be the same as the SDSS photometric measurements. The synthetic and photometric measurements agree within ~ 0.1 mag for the objects observed in photometric nights. This scatter is due to both the uncertainties in the SDSS photometric zeropoints (5 – 10%, see §2) and the spectroscopic observations. Therefore, the absolute flux scale in Figure 3 is only accurate to ~ 0.1 mag.

The emission line properties of the quasars are listed in Table 3. Central wavelengths and rest frame equivalent widths of five major emission lines are measured following the procedures of Paper I. Table 4 gives the continuum properties of the quasars. As in Paper I, redshifts are determined from all emission lines redward of Lyα; Lyα itself is not used, due to absorption from the Lyα forest on its blue side. The AB magnitude of the quasar continuum at 1450 Å (rest frame), AB_{1450}, is determined by the average flux in the continuum window from 1425 Å to 1475 Å (rest frame) from the spectra in Figure 3. The absolute magnitude M_B is determined by assuming a cosmology of $q_0 = 0.5$, $h = 0.5$, and a power law index of –0.5 following Schneider, Schmidt & Gunn (1991). The AB_{1450} and M_B magnitudes are corrected for Galactic extinction using the reddening map of Schlegel, Finkbeiner & Davis (1998); these values are accurate to ~ 0.1 mag, due to the uncertainties in the absolute flux scale (see above). The emission and absorption properties of most of these quasars are very similar to those of other quasars at similar redshift (c.f. Schneider, Schmidt & Gunn 1989, 1991, 1997, Warren *et al.* 1991, Kennefick, Djorgovski & de Carvalho 1995, Storrie-Lombardi *et al.* 1996, Paper I), with some interesting exceptions, which we now discuss.

3.1. Notes on Individual Objects

SDSSp J112253.51+005329.8 ($z = 4.57$). A number of absorption systems are present in the spectrum. In particular, the peak of the Lyα emission line is self-absorbed by several lines.

SDSSp J120441.73–002149.6 ($z = 5.03$). This is the second quasar found at $z \gtrsim 5$ in our survey. As was the case for SDSSp J033829.31–002156.3 ($z = 5.00$, Paper I), the determination of an accurate redshift is not straightforward. A straight Gaussian fit to the Lyα emission line yields a redshift of 5.14. The Si IV and C IV emissions are affected by atmospheric absorption; they give a consistent redshift of about 5.03. We therefore adopt a redshift of 5.03 ± 0.05 for this quasar. For these two $z \gtrsim 5$ quasars, the differences between the redshifts of the Lyα lines and that of the Si IV and C IV lines are about 0.1, much larger

than other quasars at $z > 4$ (Schneider, Schmidt & Gunn 1991). It is not clear whether the Lyman α absorption at the blue wing of the Lyman α emission line can fully account for this large redshift discrepancy. The Lyα line profile is also more symmetric than that of other high-redshift quasars. This object is relatively bright at $i^* = 19.3$, suitable for high signal-to-noise ratio studies of its emission line profiles.

SDSSp J130348.94+002010.4 ($z = 3.64$). This BAL quasar shows absorption troughs shortward of $z \approx 3.64$ (as measured by the emission peaks) in virtually all sampled strong emission lines, extending blueward by up to $\sim 13,000$ km s^{-1} (e.g., for C IV). Although this object is a marked outlier in SDSS colors, it is redder in $g^* - r^*$ and $i^* - z^*$ (perhaps because of the BALs) than the great majority of other known high-redshift quasars, and does not satisfy our formal selection criteria (eq. 1).

SDSSp J141205.78–010152.6 ($z = 3.73$). This object possesses an interesting absorption system at $z = 3.62$ ($v = -7000$ km s^{-1}) with absorption lines of C IV (7158Å), N V (5729Å), Lyα (5619Å) and Lyβ+O VI (4763Å). The C IV absorption has a FWHM of ~ 1300 km s^{-1}. This system is probably also responsible for the peculiar shape of the Lyman Limit System. High resolution observations are needed to determine the nature of this absorption system, especially whether it is a so-called "mini-BAL" system (defined as the velocity span of the absorption profile being narrower than 2000 km s^{-1}; Barlow, Hamann, & Sargent 1997, Churchill *et al.* 1999).

SDSSp J141315.36+000032.1 ($z = 4.08$). This object was observed under poor weather conditions, and the spectrum has a very low signal-to-noise ratio. However, the Lyα and C IV emission lines are clearly detected, and give consistent redshifts.

SDSSp J141332.35–004909.7 ($z = 4.14$). This is another mini-BAL quasar candidate. The C IV trough has a FWHM of ~ 1400 km s^{-1}. An accurate center and equivalent width of the Lyα line cannot be measured due to the presence of the BAL trough of N V, which appears blueward of the Lyα emission.

SDSSp J151618.44–000544.3 ($z = 3.70$). The spectrum of this object shows a strong damped Lyα system candidate at $z = 3.03$ with rest-frame equivalent width of ~ 38 Å. In comparison, the strongest known damped Lyα system has a rest-frame equivalent width of 41 Å (Wolfe *et al.* 1986). The spectrum at $\lambda > 7500$Å is affected by a CCD defect and is not plotted.

SDSSp J153259.96–003944.1 ($z = 4.62$). This is a unique object. Its spectrum features two breaks at 6800 Å and 5100 Å, respectively. We interpret the two breaks as the onset of the Lyman α forest and a Lyman Limit System respectively, giving a consistent redshift of $z = 4.62$. The redshifts of onset of the Lyman α forest and Lyman Limit System

are typically close to the emission line redshift for high-redshift quasars (e.g., Schneider, Schmidt & Gunn 1991, Storrie-Lombardi *et al.* 1996); we therefore adopt a redshift of 4.62 ± 0.04 for this object. However, this object has no detected emission lines. We discuss high signal-to-noise ratio Keck spectroscopy, VLA radio observations and optical broad-band polarimetry of this object in a separate paper (Fan *et al.* 1999b).

SDSSp J160501.21–011220.0 ($z = 4.92$). This object is the highest redshift BAL quasar yet discovered. It has two BAL systems in its spectrum, one at $z = 4.86$, the other at $z = 4.69$. The absorption due to the BAL systems is detected for the Lyα, N V, Si IV and C IV lines. Because of the BALs, an emission line redshift cannot be measured accurately. We adopt a redshift of 4.92 ± 0.05, as measured from the peaks of the N V, O I and Si IV lines. In Figure 4, we show the absorption systems for each line, aligned in the rest-frame velocity of the quasar. The two BALs are at relative velocities of 3000 km s^{-1} and 11,700 km s^{-1}, respectively. This is an ideal object for further spectroscopic observations to study the BAL phenomenon at very high redshift. The presence of the BALs affects the broad-band colors, resulting in $r^* - i^* \sim 3$, compared to $r^* - i^* < 2$ for other $z \sim 5$ quasars (Figure 1c).

SDSSp J162116.91–004251.1 ($z = 3.70$). This is a very bright high-redshift quasar ($i^* = 17.23$, $M_B = -28.81$), the most luminous we have yet found. The signal-to-noise ratio of this spectrum is high, allowing identification of several absorption lines. It is particularly suitable for high-resolution studies of its absorption systems.

SDSSp J165527.61–000619.2 ($z = 3.99$). This object has a very strong Lyα emission line; the rest-frame equivalent width is 172 Å, which is more than twice the value of most quasars in this redshift range. The presence of this strong emission line affects the broad-band colors. It has $g^* - r^* \sim 3$, compared to $g^* - r^* \sim 1.6$ for ordinary $z \sim 4$ quasars (Figure 1b).

The Sloan Digital Sky Survey (SDSS) is a joint project of the University of Chicago, Fermilab, the Institute for Advanced Study, the Japan Participation Group, The Johns Hopkins University, the Max-Planck-Institute for Astronomy, Princeton University, the United States Naval Observatory, and the University of Washington. Apache Point Observatory, site of the SDSS, is operated by the Astrophysical Research Consortium. Funding for the project has been provided by the Alfred P. Sloan Foundation, the SDSS member institutions, the National Aeronautics and Space Administration, the National Science Foundation, the U.S. Department of Energy, and the Ministry of Education of Japan. The SDSS Web site is `http://www.sdss.org/`. XF and MAS acknowledge additional support from Research Corporation, NSF grants AST96-16901, the Princeton

University Research Board, and an Advisory Council Scholarship. DPS acknowledges the support of NSF grant AST95-09919 and AST99-00703. We thank Niel Brandt for useful discussions. We thank Karen Gloria and Russet McMillan for their usual expert help at the 3.5m telescope.

REFERENCES

Barlow, T.A., Hamann, F., & Sargent, W.L.W. 1997, in *Mass Ejection from AGN*, ASP Conference Series 128, eds N. Arav, I. Shlosman, and R.J. Weymann (PASP: San Francisco), 13

Becker, R. H., White, R. L., & Helfand, D. J., 1995, ApJ, 450, 559

Brandt, W.N. 1999, in preparation

Churchill, C.W., Schneider, D.P., Schmidt, M. & Gunn, J.E. 1999, AJ, 117, 2573

Condon, J. J., Cotton, W. D., Greisen, E. W., Yin, Q. F., Perley, R. A., Taylor, G. B., & Broderick, J. J., 1998, AJ, 115, 1693

Fabian, A.C., Brandt, W.N., McMahon, R.G., & Hook, I.M. 1997, MNRAS, 291, L5

Fan, X. 1999, AJ, 117, 2528

Fan, X. *et al.* 1999a, AJ, 118, 1 (Paper I)

Fan, X. *et al.* 1999b, ApJL, in press (astro-ph/9910001)

Fukugita, M., Ichikawa, T., Gunn, J.E., Doi, M., Shimasaku, K., & Schneider, D.P. 1996, AJ, 111, 1748

Gunn, J.E., *et al.* 1998, AJ, 116, 3040

Kennefick, J.D., Djorgovski, S.G., & de Carvalho, R.R. 1995, AJ, 110, 255

Lupton, R.H., Gunn, J.E., & Szalay, A. 1999a, AJ, 118, 1406

Lupton, R.H. *et al.* 1999b, in preparation

Moran, E.C., & Helfand, D.J. 1997, ApJ, 484, L95

Oke, J.B., 1990, AJ, 99, 1621

Oke, J.B., & Gunn, J.E. 1983, ApJ, 266, 713

Schlegel, D.J, Finkbeiner, D.P., & Davis, M. 1998, ApJ, 500, 525

Schneider, D.P., Schmidt, M. & Gunn, J.E. 1989, AJ, 89,1951

Schneider, D.P, Schmidt, M., & Gunn, J.E. 1991, AJ, 101,2004

Schneider, D.P, Schmidt, M., & Gunn, J.E. 1991, AJ, 102, 837

Schneider, D.P, Schmidt, M., & Gunn, J.E. 1997, AJ, 114, 36

Smith, J. D., Thompson, D. & Djorgovski, S., 1994, AJ, 107, 24

Siegmund, W. *et al.* 1999, in preparation

Storrie-Lombardi, L.J., McMahon, R. G., Irwin, M.J., & Hazard, C. 1996, ApJ, 468, 121

Warren, S. J., Hewett, P. C., & Osmer, P. S., 1991, ApJS, 76, 23

Wolfe, A., Turnshek, D. Smith, A. G., and Cohen, R. 1986, ApJS, 61, 249

Voges, W., *et al.* 1999, A&A, 349, 389

York, D. G., *et al.* 1999, in preparation

Table 1. Summary of SDSS Photometric Runs

Run	Date	Strip	RA Range	seeing
77	June 27 1998	North	$14^h10^m - 17^h$	$1.6'' - 1.9''$
85	June 28 1998	South	$14^h20^m - 17^h$	$1.3'' - 2.0''$
745	Mar 20 1999	North	$10^h40^m - 16^h40^m$	$1.3'' - 1.6''$
752	Mar 21 1999	South	$9^h40^m - 16^h40^m$	$1.3'' - 2.5''$

Table 2. Positions and Photometry of SDSS High-redshift Quasars

SDSS name	redshift	u^*	g^*	r^*	i^*	z^*	run
SDSSp J105320.43 − 001649.3[a]	4.29 ± 0.01	23.81 ± 0.43	21.75 ± 0.07	19.36 ± 0.02	19.32 ± 0.02	19.33 ± 0.07	752
SDSSp J111246.30 + 004957.5[b]	3.92 ± 0.01	24.19 ± 0.36	20.09 ± 0.02	18.82 ± 0.01	18.69 ± 0.01	18.64 ± 0.04	752
SDSSp J111401.48 − 005321.1	4.58 ± 0.01	23.42 ± 0.23	22.94 ± 0.11	20.64 ± 0.03	19.60 ± 0.02	19.56 ± 0.06	745
SDSSp J112253.51 + 005329.8	4.57 ± 0.02	23.45 ± 0.46	22.78 ± 0.22	20.21 ± 0.03	19.11 ± 0.02	19.11 ± 0.07	752
SDSSp J120441.73 − 002149.6	5.03 ± 0.05	22.29 ± 0.21	24.92 ± 0.01	20.82 ± 0.06	19.31 ± 0.02	19.12 ± 0.08	752
SDSSp J122600.68 + 005923.6	4.25 ± 0.02	23.00 ± 0.32	21.26 ± 0.05	19.01 ± 0.01	18.91 ± 0.02	18.86 ± 0.05	752
SDSSp J123503.04 − 000331.8	4.69 ± 0.01	23.58 ± 0.23	23.85 ± 0.28	21.49 ± 0.06	20.11 ± 0.03	20.05 ± 0.09	745
SDSSp J130348.94 + 002010.5[c]	3.64 ± 0.03	23.22 ± 0.25	20.94 ± 0.03	18.93 ± 0.01	18.71 ± 0.01	18.25 ± 0.03	745
SDSSp J131052.52 − 005533.4	4.14 ± 0.01	23.28 ± 0.49	20.85 ± 0.02	18.85 ± 0.01	18.82 ± 0.01	18.88 ± 0.03	745
SDSSp J132110.82 + 003821.7	4.70 ± 0.01	23.67 ± 0.24	23.49 ± 0.19	21.40 ± 0.06	20.01 ± 0.03	20.17 ± 0.09	745
SDSSp J141205.78 − 010152.6	3.73 ± 0.02	24.09 ± 0.37	20.58 ± 0.02	19.39 ± 0.02	19.22 ± 0.02	19.02 ± 0.06	77
SDSSp J141315.36 + 000032.1	4.08 ± 0.02	23.61 ± 0.34	21.46 ± 0.05	19.74 ± 0.02	19.72 ± 0.03	19.77 ± 0.10	752
SDSSp J141332.35 − 004909.7	4.14 ± 0.01	24.11 ± 1.62[d]	21.11 ± 0.04	19.59 ± 0.02	19.29 ± 0.02	19.17 ± 0.06	752
SDSSp J142329.98 + 004138.4	3.76 ± 0.01	23.54 ± 0.33	20.77 ± 0.03	19.55 ± 0.02	19.52± 0.03	19.56 ± 0.08	77
SDSSp J142647.82 + 002740.4	3.69 ± 0.01	22.45 ± 0.13	20.55 ± 0.02	19.40 ± 0.01	19.34 ± 0.02	19.28 ± 0.05	85
SDSSp J144428.67 − 012344.1	4.16 ± 0.01	23.37 ± 0.35	21.24 ± 0.04	19.52 ± 0.02	19.47 ± 0.02	19.37 ± 0.07	85
SDSSp J144758.46 − 005055.4	3.80 ± 0.01	23.50 ± 0.26	20.98 ± 0.03	19.58 ± 0.02	19.37 ± 0.02	19.14 ± 0.07	77
SDSSp J151618.44 − 000544.3	3.70 ± 0.01	24.10 ± 0.31	21.85 ± 0.08	20.18 ± 0.02	19.99 ± 0.03	19.90 ± 0.12	752
SDSSp J152740.52 − 010602.6	4.41 ± 0.02	23.98 ± 0.14	22.78 ± 0.13	20.46 ± 0.03	19.92 ± 0.03	19.67 ± 0.08	752
SDSSp J153259.96 − 003944.1	4.62 ± 0.04	23.74 ± 0.36	23.78 ± 0.30	21.15 ± 0.05	19.75 ± 0.03	19.55 ± 0.07	77
SDSSp J160501.21 − 011220.0	4.92 ± 0.05	24.08 ± 0.36	25.04 ± 0.49	22.50 ± 0.17	19.78 ± 0.03	19.92 ± 0.10	85
SDSSp J161926.87 − 011825.2	3.84 ± 0.01	22.77 ± 0.24	21.80 ± 0.07	20.17 ± 0.03	19.93 ± 0.03	20.02 ± 0.13	85
SDSSp J162116.91 − 004251.1	3.70 ± 0.01	22.09 ± 0.11	18.62 ± 1.09[d]	17.28 ± 0.00	17.23 ± 0.00	17.26 ± 0.01	752
SDSSp J165527.61 − 000619.2	3.99 ± 0.01	24.57 ± 0.21	22.92± 0.17	20.05 ± 0.02	20.16 ± 0.04	20.17 ± 0.15	77

Positions are in J2000.0 coordinates; asinh magnitudes (Lupton, Gunn & Szalay 1999) are quoted; errors are statistical only. For reference, zero flux corresponds to asinh magnitudes of 23.40, 24.22, 23.98, 23.51, and 21.83 in u^*, g^*, r^*, i^*, and z^*, respectively.

[a]This is the previously known quasar BRI1050–0000 (Storrie-Lombardi *et al.* 1996).

[b]This is the previously known quasar BRI1110+0106 (Smith, Thompson & Djorgovski 1994).

[c]This object does not satisfy the color selection criteria (eq. 1).

[d]The large magnitude error indicates that the magnitude is not to be trusted.

Table 3. Emission Line Properties of SDSS High-redshift Quasars

quasar	O VI 1034	Lyα 1216+1240	O I+Si II 1306	Si IV+O IV] 1402	C IV 1549
SDSSp J111401.48-005321.1		6841 ± 4		7822 ± 16	8642 ± 18
		47.6 ± 3.8		14.3 ± 2.1	28.4 ± 3.6
SDSSp J112253.51+005329.8		6797 ± 2	7290 ± 4	7804 ± 6	8607 ± 3
		96.0 ± 1.4	3.4 ± 0.4	29.1 ± 2.3	42.7 ± 1.3
SDSSp J120441.73-002149.6		7463 ± 3		8450 ± 20	9332 ± 31
		68.0 ± 1.7		13.9 ± 2.2	28.6 ± 6.1
SDSSp J122600.68+005923.6		6210 ± 0	6846 ± 12	7369 ± 8	8156 ± 2
		88.8 ± 2.2	4.7 ± 0.9	7.1 ± 1.1	23.7 ± 1.0
SDSSp J123503.04-000331.8	5883 ± 6	6927 ± 1	7434 ± 16	7960 ± 34	8807 ± 13
	31.3 ± 6.1	85.8 ± 8.1	6.7 ± 2.2	10.6 ± 5.1	29.4 ± 5.0
SDSSp J131052.52-005533.4		6267 ± 1			7973 ± 3
		71.3 ± 2.9			28.5 ± 1.2
SDSSp J132110.82+003821.7		6967 ± 2			8830 ± 5
		42.8 ± 5.6			34.8 ± 6.4
SDSSp J141205.78-010152.6		5779 ± 2	6200 ± 12	6637 ± 13	7304 ± 14
		79.7 ± 4.3	2.0 ± 0.9	8.1 ± 1.3	13.6 ± 2.5
SDSSp J141332.35-004909.7	5315 ± 2			7197 ± 15	7971 ± 2
	19.9 ± 1.3			11.7 ± 1.9	28.3 ± 1.4
SDSSp J141315.36+000032.1		6183 ± 1			7875 ± 4
		69.8 ± 4.1			22.6 ± 4.6
SDSSp J142329.98+004138.4		5843 ± 4		6679 ± 9	7374 ± 3
		50.9 ± 2.8		11.2 ± 1.2	32.4 ± 1.4
SDSSp J142647.82+002740.4	4860 ± 4	5727 ± 1		6388 ± 16	7265 ± 4
	26.3 ± 1.5	48.4 ± 4.3		10.8 ± 2.6	26.9 ± 1.5
SDSSp J144428.67-012344.1		6358 ± 4		7243 ± 26	7999 ± 12
		76.3 ± 4.9		13.3 ± 5.1	37.2 ± 2.9
SDSSp J144713.08-012158.7		5897 ± 3		6736 ± 7	7424 ± 6
		37.9 ± 4.7		16.8 ± 1.2	30.1 ± 1.5
SDSSp J151618.44-000544.3		5805 ± 12		6576 ± 13	7299 ± 12
		85.8 ± 16.2		34.3 ± 3.3	42.3 ± 3.4
SDSSp J152740.52-010602.6		6595 ± 2		7584 ± 4	
		74.1 ± 4.7		7.2 ± 1.6	
SDSSp J161926.87-011825.2		5891 ± 3		6792 ± 15	7491 ± 5
		69.0 ± 6.2		15.7 ± 1.9	36.2 ± 1.8
SDSSp J162116.91-004251.1	4853 ± 6	5731 ± 0	6146 ± 4	6589 ± 6	7288 ± 2
	19.4 ± 2.0	82.3 ± 1.6	6.2 ± 0.6	7.2 ± 0.7	43.8 ± 1.0
SDSSp J165527.61-000619.2		6061 ± 1	6512 ± 10		7740 ± 4
		172.0 ± 6.0	14.6 ± 3.0		63.3 ± 3.5

The two entries in each line are the central wavelength and rest frame equivalent width from the Gaussian fit to the line profile, both measured in Ångstroms.

Emission line properties are not measured for SDSSp J130348.94+002010.5, SDSSp J153259.96–003944.1 or SDSSp J160501.21–011220.0.

Table 4. Continuum Properties of SDSS High-redshift Quasars

quasar	redshift	E(B–V)	AB^a_{1450}	M_B	z_{LLS}	z^b_{abs}
SDSSp J111401.48 − 005321.1	4.58 ± 0.01	0.038	19.73	–26.82	4.50	
SDSSp J112253.51 + 005329.8	4.57 ± 0.02	0.036	19.20	–27.35	4.48	
SDSSp J120441.73 − 002149.6	5.03 ± 0.05	0.026	19.05	–27.64		
SDSSp J122600.68 + 005923.6	4.25 ± 0.02	0.024	19.07	–27.36	4.10	
SDSSp J123503.04 − 000331.8	4.69 ± 0.01	0.022	20.30	–26.29	4.68	
SDSSp J130348.94 + 002010.4	3.64 ± 0.03	0.020	18.88	–27.31		
SDSSp J131052.52 − 005533.4	4.14 ± 0.01	0.025	18.93	–27.46	4.10	
SDSSp J132110.82 + 003821.7	4.70 ± 0.01	0.032	20.12	–26.47	4.59	
SDSSp J141205.78 − 010152.6	3.73 ± 0.02	0.057	19.32	–26.91	3.62	3.26
SDSSp J141315.36 + 000032.1	4.08 ± 0.02	0.048	20.07	–26.30		
SDSSp J141332.35 − 004909.7	4.14 ± 0.01	0.043	19.29	–27.10		
SDSSp J142329.98 + 004138.4	3.76 ± 0.01	0.027	19.75	–26.49	3.59	
SDSSp J142647.82 + 002740.4	3.69 ± 0.01	0.031	19.53	–26.69		
SDSSp J144428.67 − 012344.1	4.16 ± 0.01	0.047	19.60	–26.80	4.06	
SDSSp J144758.46 − 005055.4	3.80 ± 0.01	0.046	19.64	–26.62	3.53	
SDSSp J151618.44 − 000544.3	3.70 ± 0.01	0.057	20.10	–26.11	3.60	3.03
SDSSp J152740.52 − 010602.6	4.41 ± 0.02	0.156	19.62	–26.87	4.35	
SDSSp J153259.96 − 003944.1	4.62 ± 0.04	0.122	19.41	–27.16	4.62	4.58
SDSSp J160501.21 − 011220.0	4.92 ± 0.05	0.199	19.43	–27.23		
SDSSp J161926.87 − 011825.2	3.84 ± 0.01	0.119	19.73	–26.54	3.63	
SDSSp J162116.91 − 004251.1	3.70 ± 0.01	0.098	17.41	–28.81		
SDSSp J165527.61 − 000619.2	3.99 ± 0.01	0.307	20.01	–26.33		

Absolute magnitudes assume $H_0 = 50\,\mathrm{km\,s^{-1}\,Mpc^{-1}}$, $q_0 = 0.5$ and power law index $\alpha = -0.5$.

[a]The absolute flux calibration is accurate to ~ 0.1 mag.

[b]These are redshifts of candidate damped Lyα lines seen in the spectra.

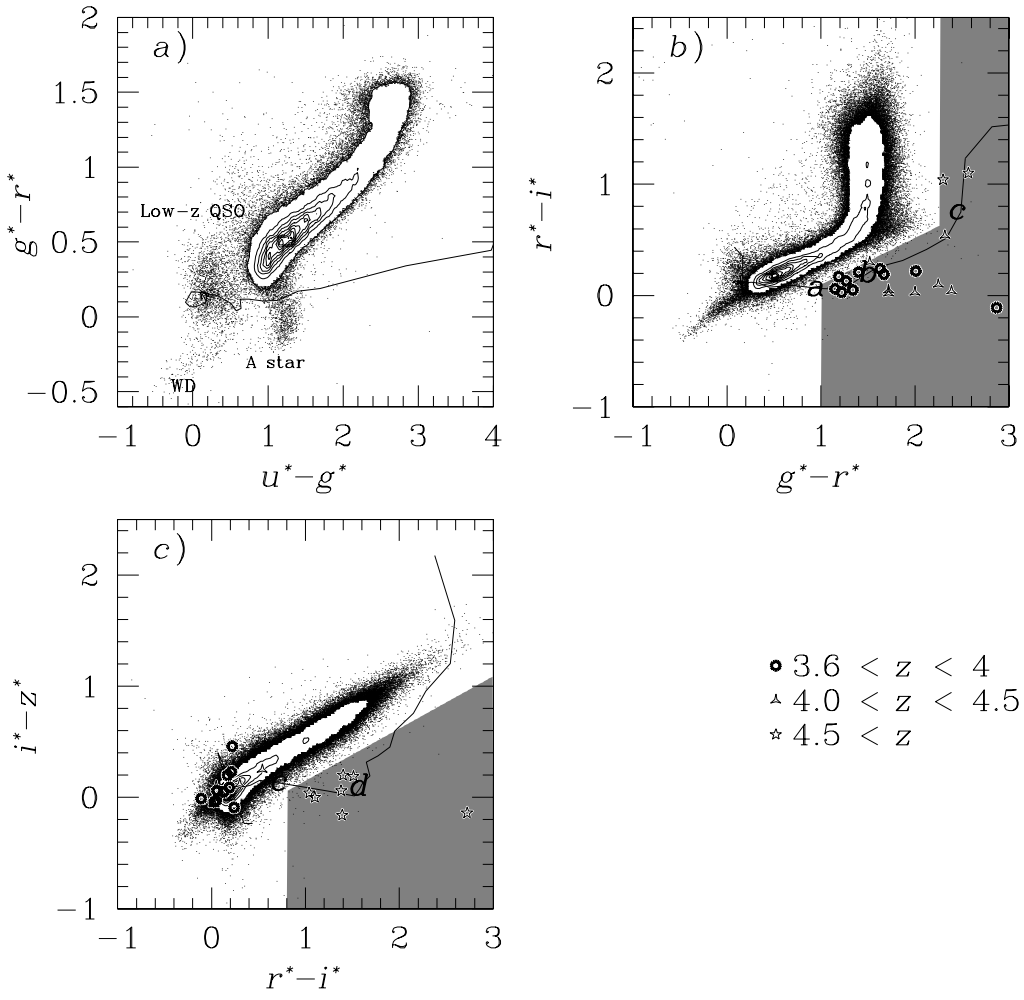

Figure 1. Color-color diagrams for all stellar objects in 75 square degrees of SDSS imaging data from Run 752, with $i^* < 20.2$. The inner parts of the diagrams are shown as contours, linearly spaced in the density of stars in color-color space. The shaded areas on the $g^* - r^*$ vs. $r^* - i^*$ and the $r^* - i^*$ vs. $i^* - z^*$ diagrams represent the selection criteria used to select quasar candidates. The solid line is the median track of simulated quasar colors as a function of redshift (adapted from Fan 1999). The letters *a*, *b*, *c*, and *d* indicate the positions on the locus of median color quasars at $z = 3.6, 4.1, 4.6$, and 5.0, respectively. Colors of the 24 confirmed SDSS quasars at $z > 3.6$ are also plotted on the diagrams.

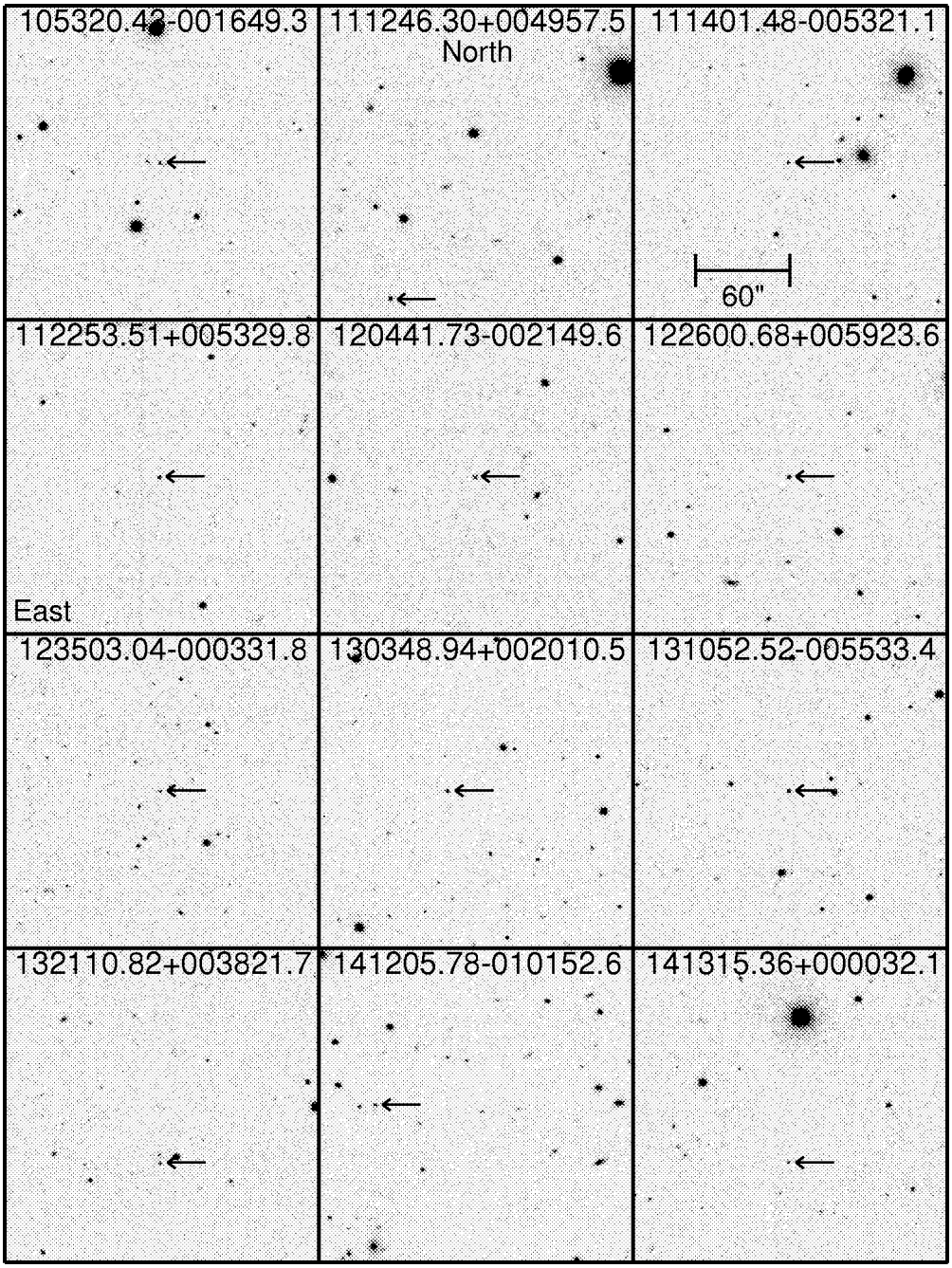

Figure 2. Finding charts for the 24 SDSS quasars. The data are $200'' \times 200''$ SDSS images in the i' band (54.1 sec exposure time). Most of them are re-constructed from the atlas images and binned background from the SDSS database (Lupton *et al.* 1999b). North is up; East is to the left.

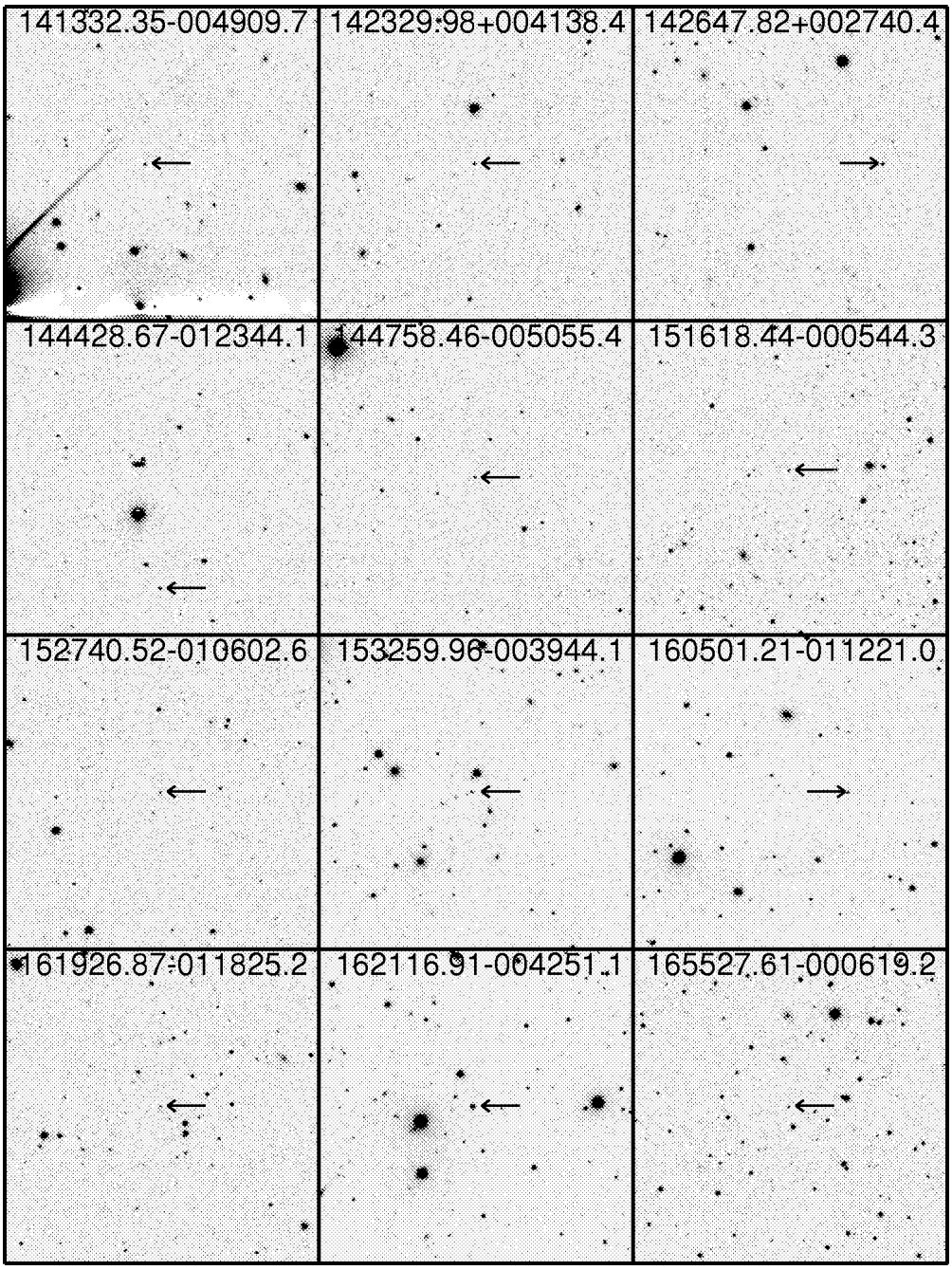

Figure 2. Continued.

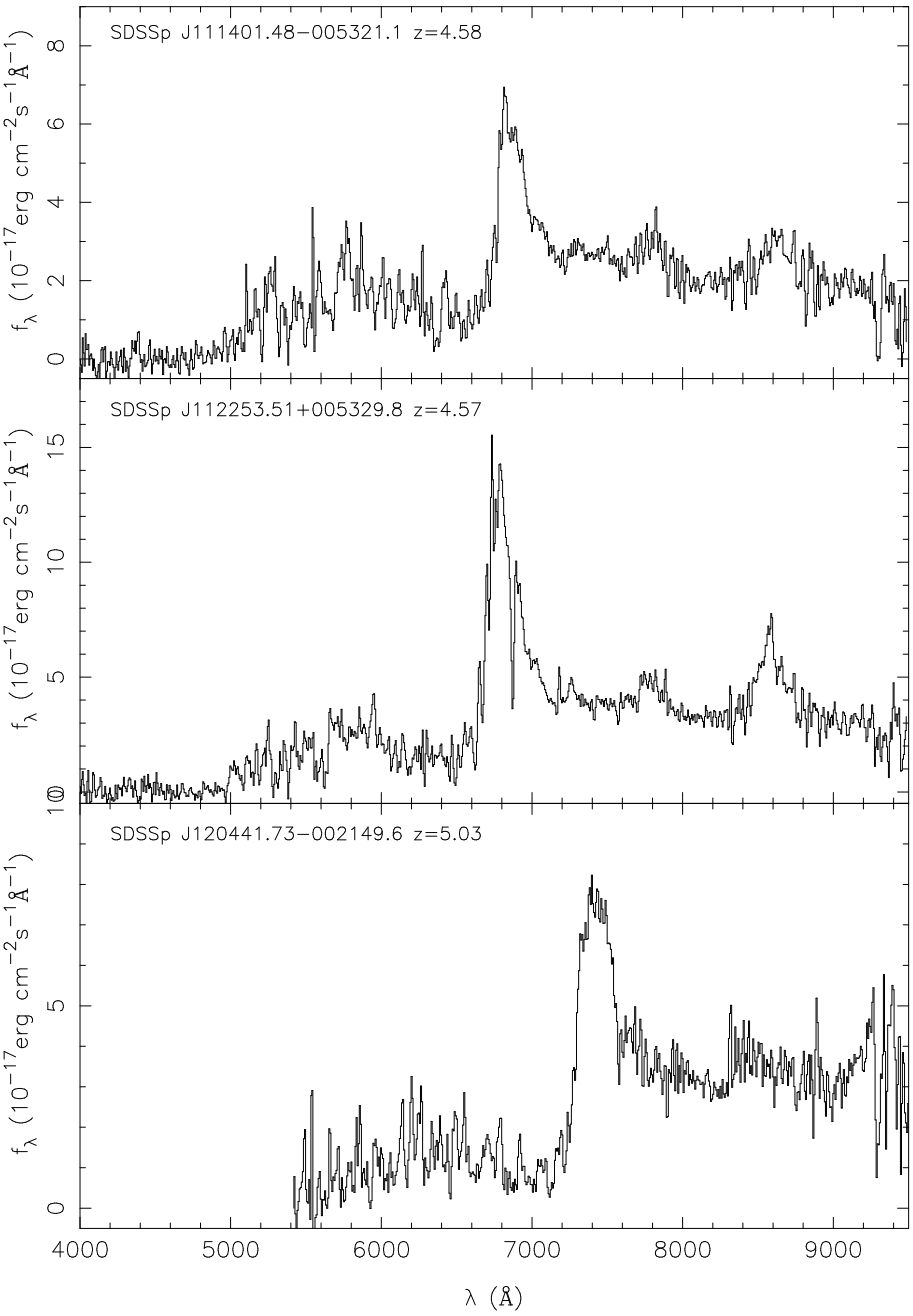

Figure 3. ARC 3.5m/DIS spectra of 22 new SDSS quasars. The spectral resolution is about 12 Å in the blue and 14 Å in the red. Each pixel represents 6.2Å. Exposure times ranged from 600 sec to 5400 sec.

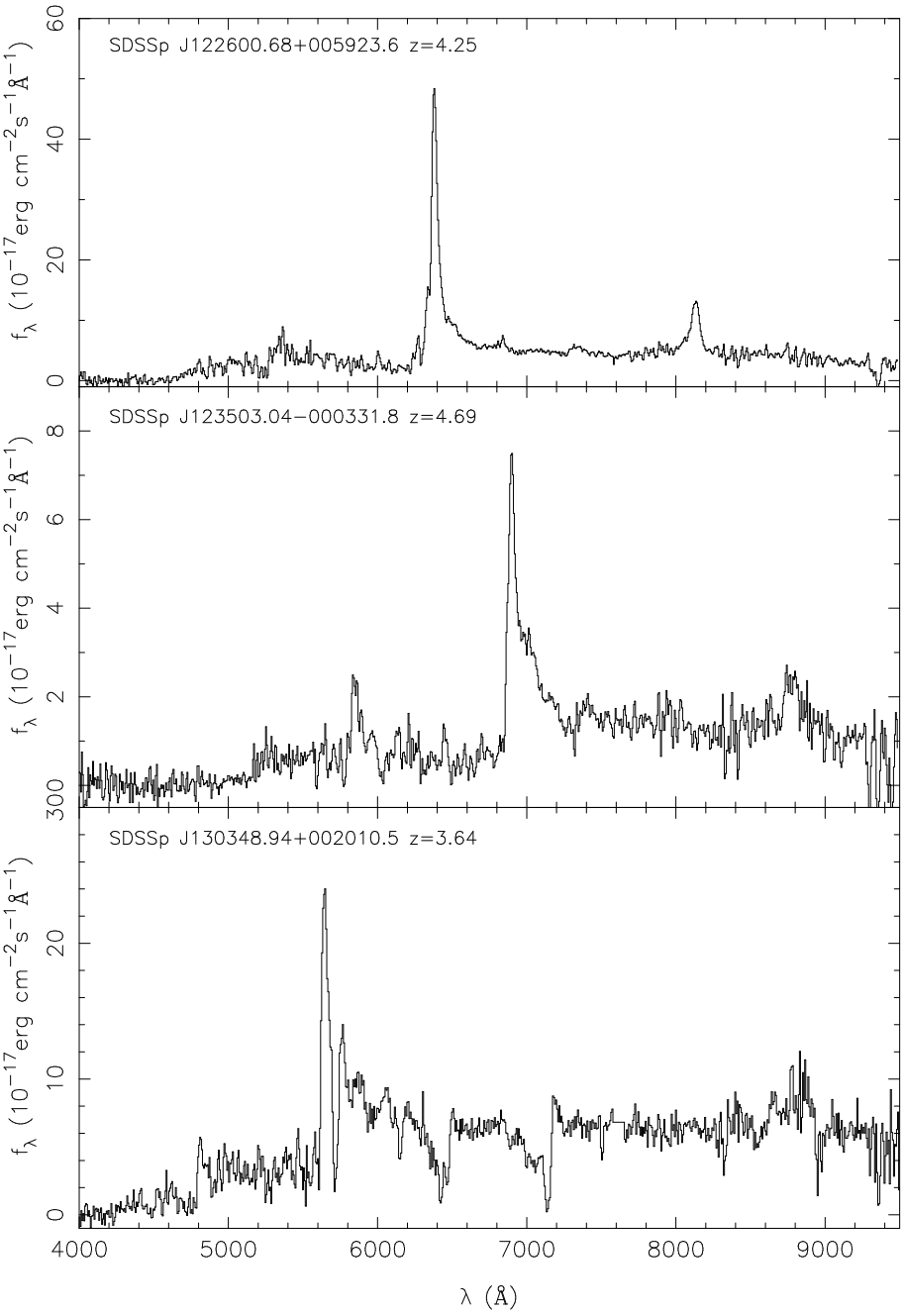

Figure 3. Continued.

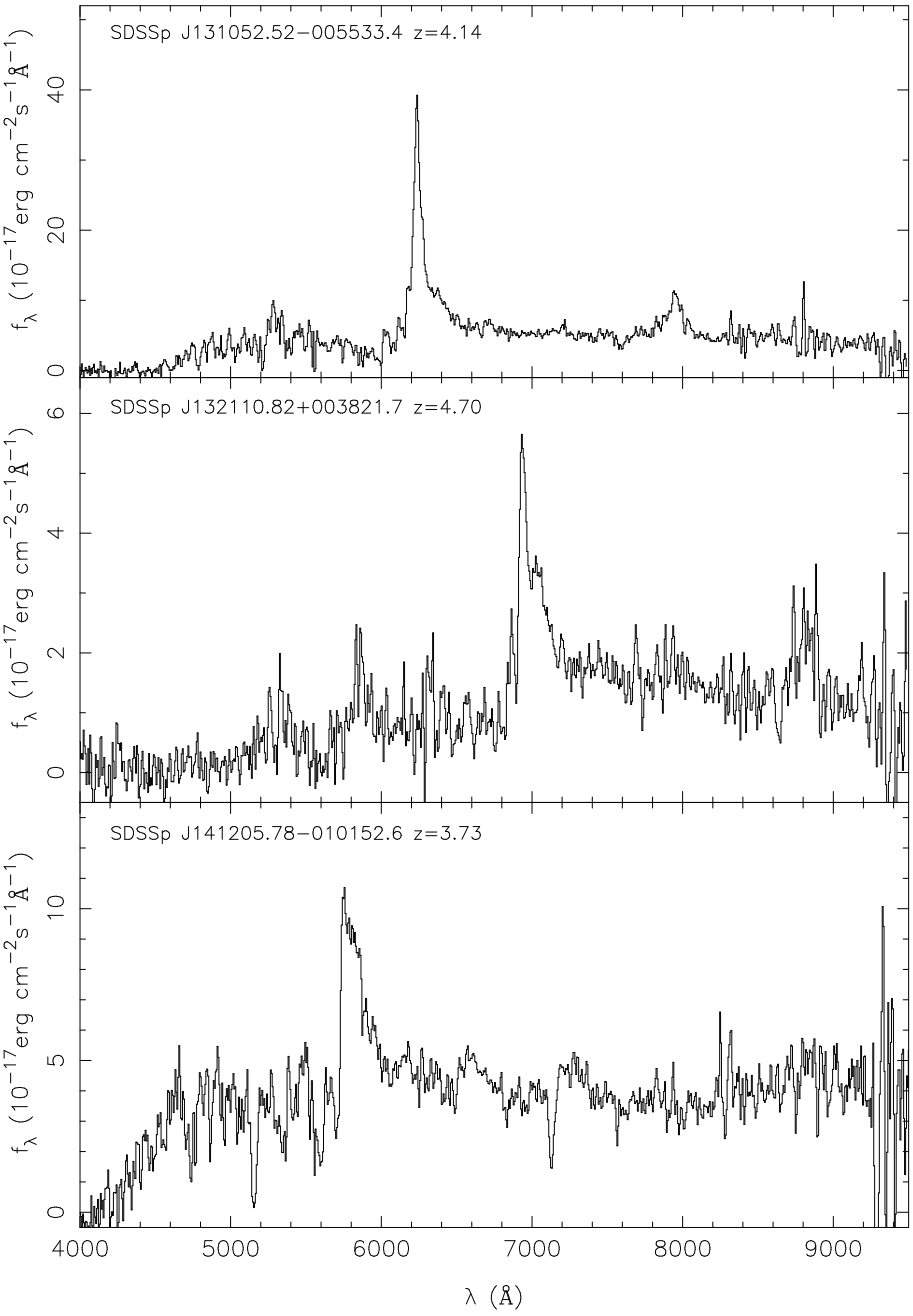

Figure 3. Continued.

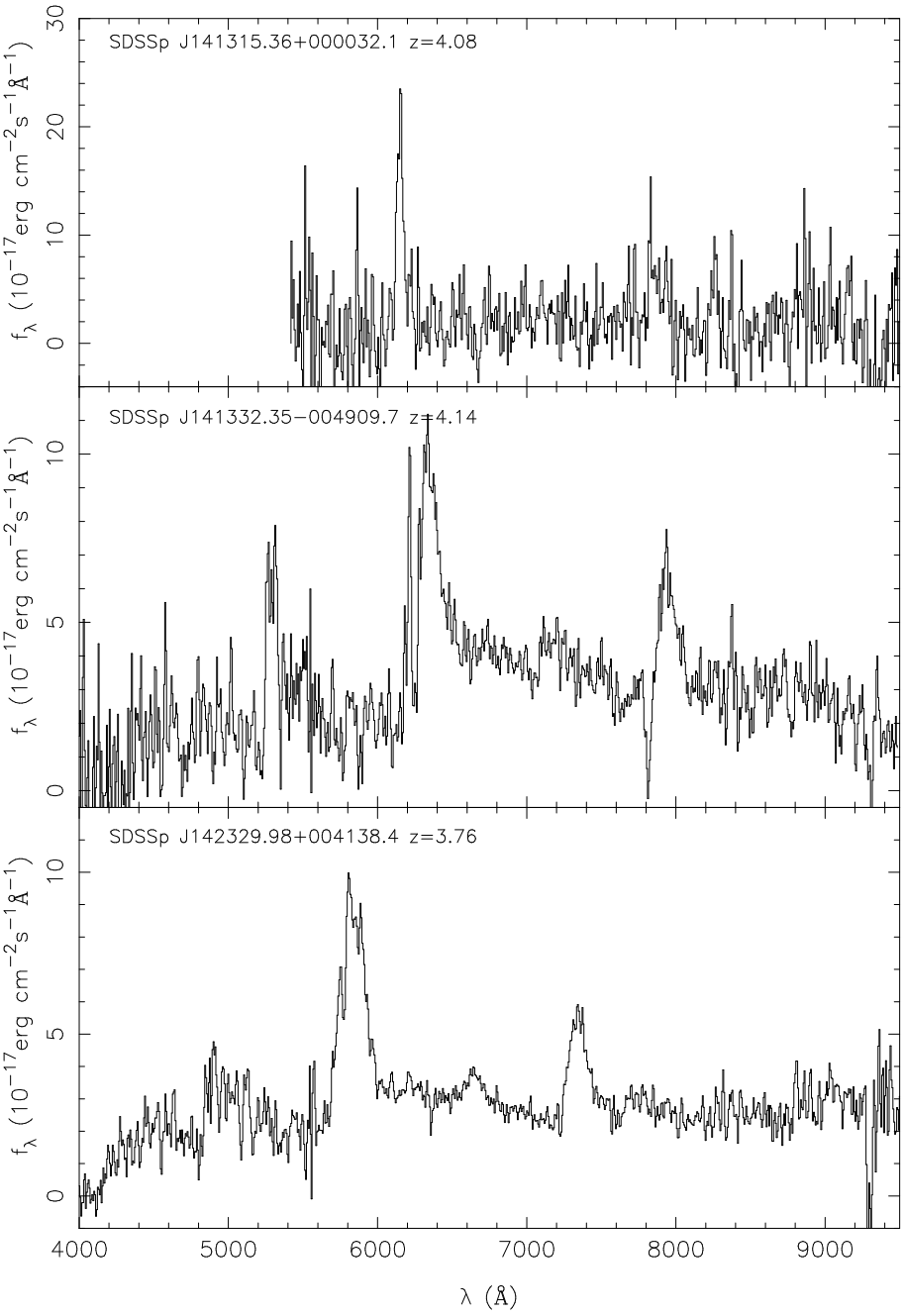

Figure 3. Continued.

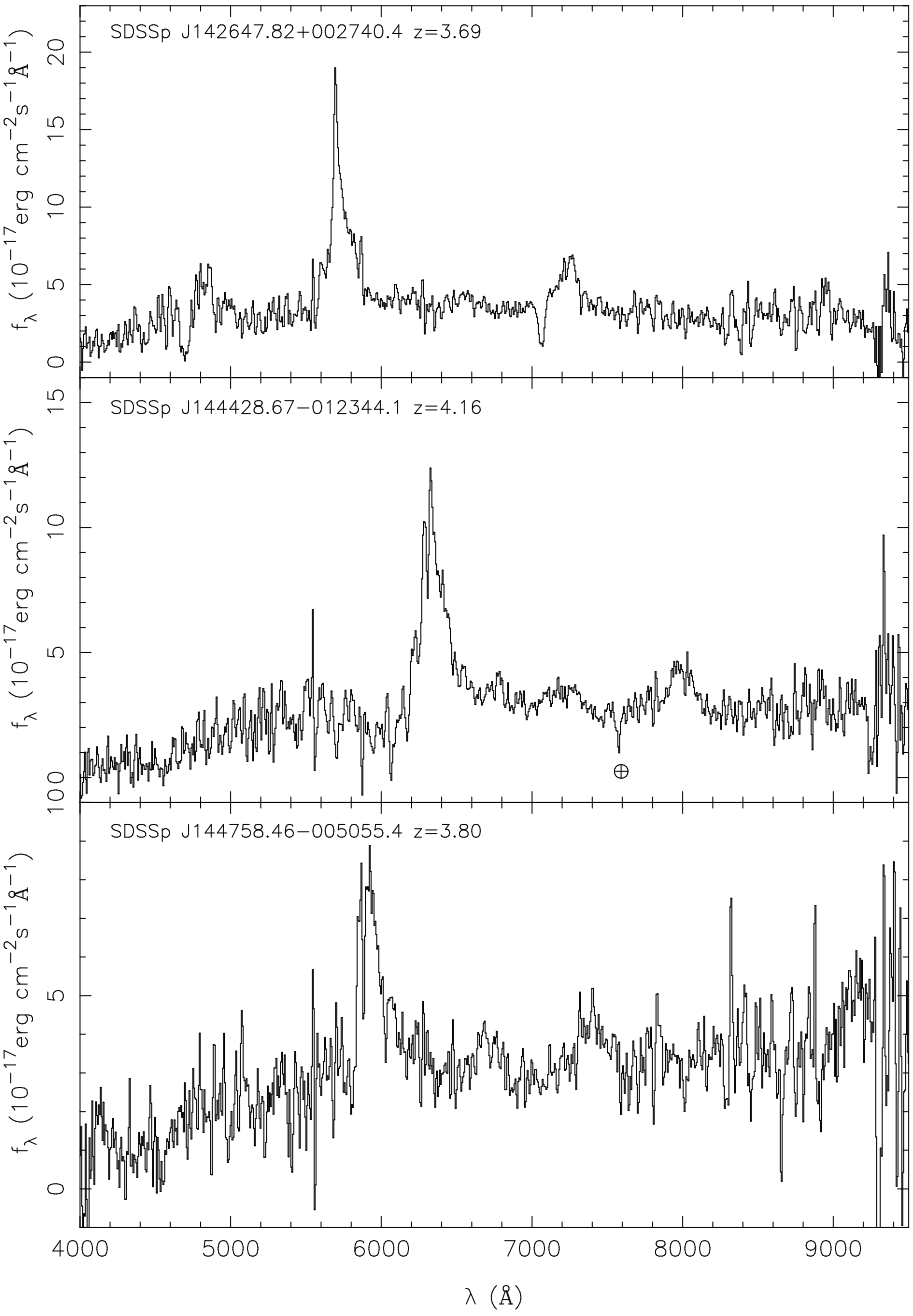

Figure 3. Continued.

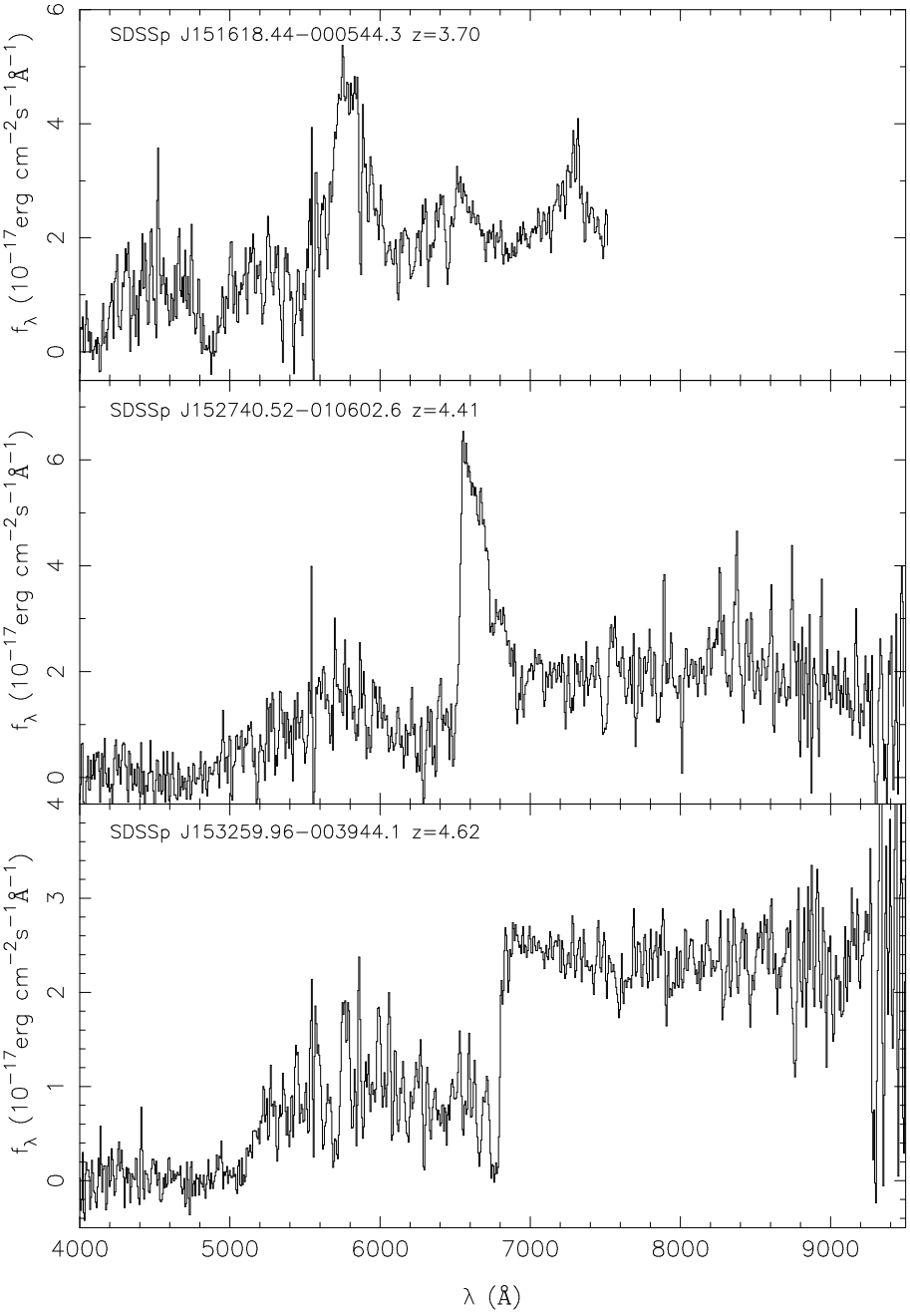

Figure 3. Continued.

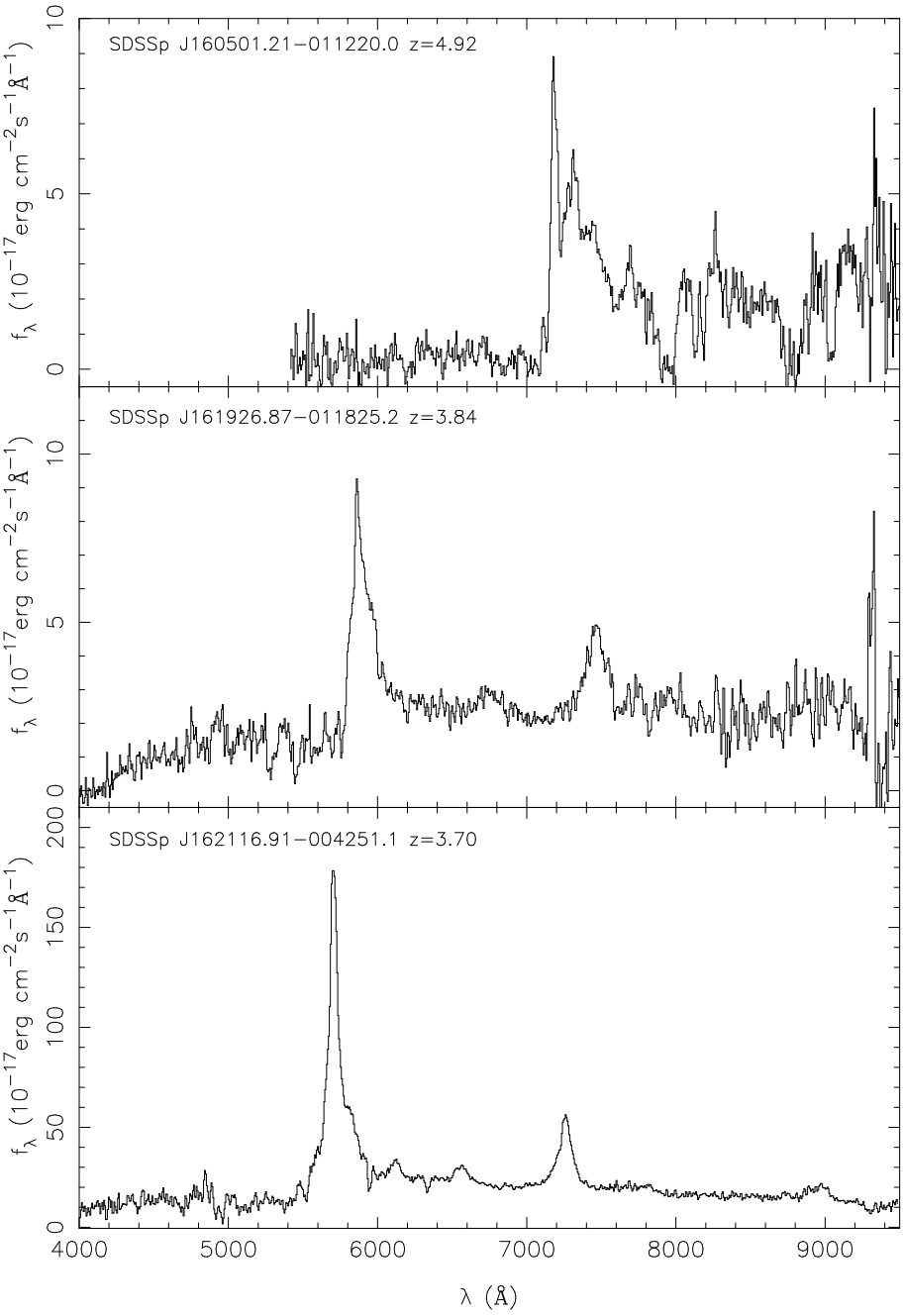

Figure 3. Continued.

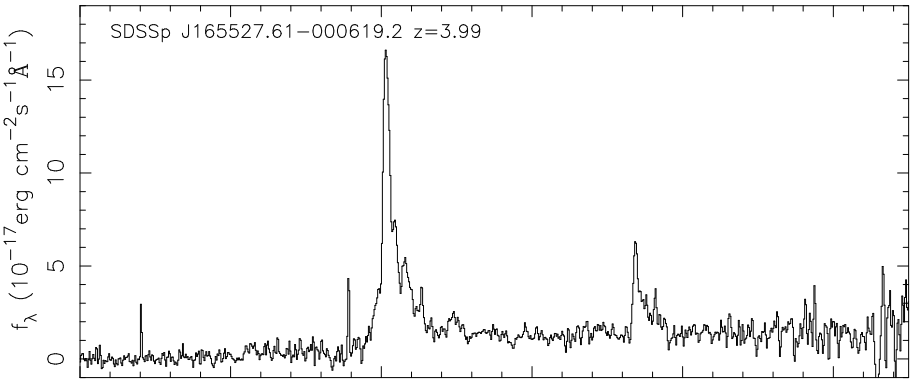

Figure 3. Continued.

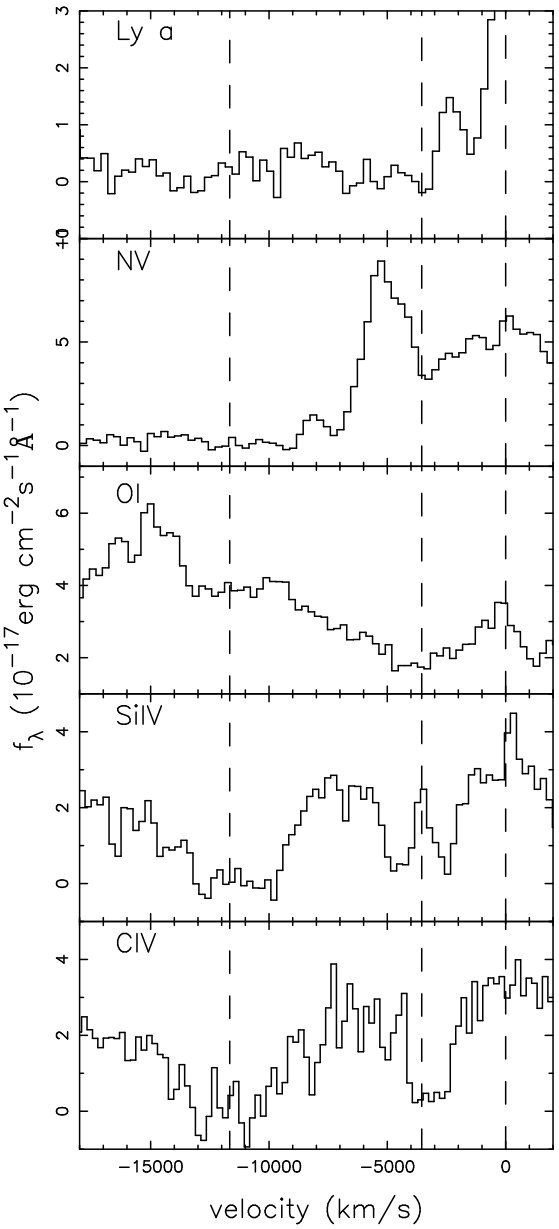

Figure 4. The Broad Absorption Lines of SDSSp J160501.21–011220.0. Absorption lines of Lyα, N V, O I, Si IV and C IV are shown, although both systems are not seen in every line. The spectra are aligned in velocity space relative to the emission line redshift of the quasar ($z = 4.92$). The velocity resolution is about 500 km s^{-1}. Two BALs are seen, one at $z = 4.86$ ($v = -3000$ km s^{-1}), and the other at $z = 4.69$ ($v = -11700$ km s^{-1}).